sciendo

**Civil and Environmental Engineering**
**Vol. 18, Issue 2, 472-481, DOI: 10.2478/cee-2022-0044**

# CROSS-SECTION SIZE OPTIMIZATION OF COLD-FORMED STEEL LIPPED CHANNEL STRUCTURAL MEMBERS SUBJECTED TO AXIAL COMPRESSION

Vitalina YURCHENKO[1,*], Anatoly PERELMUTER[2], Ivan PELESHKO[3]

[1] Chair of Steel and Timber Structures, Department of Civil Engineering, Kyiv National University of Civil Engineering and Architecture, 31 Povitroflotsky av., 03680 Kyiv, Ukraine.
[2] SCAD Soft Ltd, 3A Osvity str., of. 2, 03037 Kyiv, Ukraine.
[3] Department of Building Production, Institute of Civil Engineering and Building Systems, Lviv Polytechnic National University, 6 Karpinskoho St., Building 2, 79013 Lviv, Ukraine.
[*] corresponding author: iurchenko.vv@knuba.edu.ua

**Abstract**

A parametric optimization problem of cross-sectional sizes for cold-formed steel lipped channel structural members subjected to axial compression has been considered by the paper. An optimization problem is formulated to define optimum cross-sectional sizes of cold-formed structural member taking into account post-buckling behavior and structural requirements when stripe width, profile thickness and profile type are constant and specified in advance. Maximization of the load-carrying capacity of the cold-formed structural member has been assumed as purpose function. As optimization results cold-formed steel lipped channels with optimum dimensions have been obtained. Steel lipped channels structural members with the optimum cross-sectional dimensions have higher load-carrying capacities at the same material consumption (stripe width) comparing with the ones proposed by the manufacturer when the material consumption.

**Keywords:**

Cold-formed steel;
Buckling resistance;
Torsional-flexural buckling;
Parametric optimization;
Gradient-based methods.

## 1 Introduction

Previously, the use of cold-formed thin-walled profiles was limited to cases where reducing the weight of the structure was a priority, such as in the aviation or automotive industries. However, due to the development of production technology, corrosion protection, product availability as well as implementation of the design code the use of thin-walled structural elements, including cold-formed profiles is gradually expanding [1].

Today, various structural systems made from cold-formed steel (CFS) structural members used widely in the construction industry are imported intensively to the Ukrainian market of steel structures. Implementation of steel structures made from thin-walled cold-formed profiles in building practice is relevant and economically reasonable. There are specific fields of application where their efficiency is the highest. However, the widespread application of the structures made from thin-walled cold-formed profiles of the domestic production is delayed due to the lack of domestic experience in economic and reliable design of such structures [1].

In the papers [2] the authors said that “A high degree of flexibility in the manufacturing of various cross-sectional shapes provides a unique opportunity to further improve the load-carrying capacity of these structural elements through an optimization process, leading to more efficient and economical structural systems”. A brief review of optimization problem formulation, calculation techniques and algorithms, including gradient-based methods, stochastic search, artificial intelligent methods, and ant colony methods, have been discussed in the paper [3]. The optimization methodologies for CFS structural members have been also summarized and presented systematically in the paper [4].

Lots of papers presented the results of shape optimization of cold-formed steel columns (see for example [5, 6]). In the paper [7] the optimization problem formulation included fabrication and

© Author(s) 2022. This work is distributed under the Creative Commons BY 4.0 license (https://creativecommons.org/licenses/by/4.0/).

geometric enduse constraints. Shape optimisation of manufacturable and usable cold-formed steel singly-symmetric and open columns has been also considered by the paper [8].

An optimization methodology intended to find the optimum cross-section sizes for CFS beam structural members with maximum flexural resistance has been provided by the paper [9]. Geometrical requirements according to EuroCode 3 as well as a number of manufacturing and practical constraints have been considered in scope of the optimization procedure. The flexural resistance of the CFS structural members has been determined based on the effective width approach regulated by EuroCode. The proposed optimization procedure has been performed based on the particle swarm optimization method.

In the paper [10] authors considered the optimal design problems for cold-formed steel lipped channel beams subjected to combined action of bending, shear, and web crippling. CFS beam structural member has been also considered by the papers [11, 12] where Big Bang-Big Crunch optimization and micro Genetic Algorithm have been used. In the paper [13] authors used the particle swarm optimization method in order to obtain optimum cross-section dimensions for lipped channels, folded-flanges, and super-sigma profiles used in modular building applications as beam structural members. Comparing to the conventional CFS sections the load-carrying flexural capacity of the structural members with optimum cross-sectional sizes has been improved significantly.

In the paper [2] a practical optimization methodology for the CFS beam-column structural members with different design lengths and thicknesses, subjected to various combinations of longitudinal force and bending moment has been proposed. The optimization procedure has been performed using a genetic algorithm, when the optimization problem has been formulated as maximization the buckling resistances of CFS structural members with specified and constant material consumption.

The paper [14] presents an optimization procedure to obtain optimum dimensions for CFS channel cross-sections in structural members subjected to compression or bending. An optimization problem has been formulated as maximization of the load-carrying capacity and solved using genetic algorithms. Optimization has been performed for the different column design lengths taking into account the shift of the centroid of its effective cross-sections caused by the local buckling effects.

The paper [15] has been devoted to the shape optimization of cold-formed steel beam-columns with practical and manufacturing constraints. CFS beam-column structural member has been also considered by the papers [16, 17] in scope of unconstrained and constrained optimization procedures.

Particular attention has been paid to the optimal folding of the CFS structural members. In the paper [1] a parametric optimization problem for single edge fold size in CFS structural members subjected to axial compression has been considered. The purpose function and constraints of the mathematical model has been formulated as continuously differentiable functions, then the parametric optimization problems has been successfully solved using the gradient projection non-linear methods [18]. Additionally, a sensitivity analysis as useful optional feature that has been used in scope of the numerical algorithms developed based on the gradients methods [19].

In order to increase the widespread application of the structures made from CFS profiles of the domestic production, effective national ranges of assortments of CFS profiles have to be developed. In this paper, CFS lipped channel structural members subjected to axial compression are considered as research object, which investigated for the searching for optimum cross-sectional dimensions. The following *research tasks* are formulated: to develop a mathematical model and a numerical technique to solve an optimization problem for cross-sectional sizes of CFS structural members; to perform numerical investigations in order to obtain optimal solutions for considered research object; to develop a guide for designers relating to the optimum material distribution in the cross-sections of the CFS structural members.

## 2 Problem formulation

Applied optimum design problems for structures in some cases are formulated as parametric optimization problems, namely as searching problems for unknown structural parameters, which provide an extreme value of the specified purpose function in the feasible region defined by the specified constraints [20]. The mathematical model of the parametric optimization problems includes a set of design variables, an objective function, as well as constraints, which reflect generally non-linear dependences between them [21].

Let formulate a parametric optimization problem as follow: to find optimum values of cross-sectional sizes for CFS lipped channel structural members subjected to axial compression when the

profile perimeter (strip width), profile thickness, steel properties as well as design lengths of the structural member are constant and specified in advance.

The formulated parametric optimization problem can be stated in the following mathematical terms: to find unknown structural parameters:

$$\vec{X} = \{X_t\}^T,\ t = \overline{1, N_x}\ , \tag{1}$$

providing the maximum value of the determined objective function:

$$f^* = f(\vec{X}^*) = \max_{\vec{X} \in \Im} f(\vec{X}), \tag{2}$$

in a feasible region (search space) $\Im$ defined by the following system of constraints:

$$\varphi\ (\vec{X}) = \{\emptyset_\eta(\vec{X}) \le 0 | \eta = \overline{1, N_{IC}}\}\ , \tag{3}$$

where $\vec{X}$ is the vector of the design variables (unknown structural parameters); $N_X$ is the total number of the design variables; $f$, $\varphi_\eta$ are the continuous functions of the vector argument; $\vec{X}^*$ is the optimum solution or optimum point (the vector of optimum values of the structural parameters); $f^*$ is the optimum value of the optimum criterion (objective function); $N_{IC}$ is the number of constraints-inequalities $\varphi_\eta(\vec{X})$, which define a feasible region in the design space $\Im$.

Overall cross-section dimensions of a CFS lipped channel, namely web height *h*, flange width *b* and single edge fold length *c* (Fig. 1) are considered as design variables. Initial data for optimization are profile thickness *t*, internal bend radius *r* = 1.5*t*, material properties (base yield strength $f_{yb}$ and modulus of elasticity *E*), design lengths of the structural member corresponded to the flexural buckling modes $l_{ef,y}$ , $l_{ef,z}$. The torsional buckling length $l_{ef,T}$ is equals to the flexural buckling length $l_{ef,z}$.

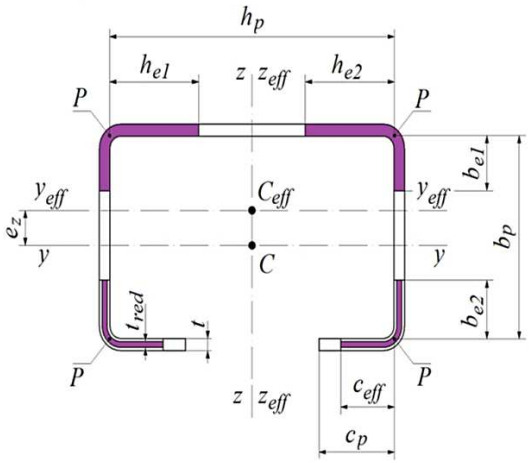



Fig. 1: Cross-section of the CFS lipped channel structural member.

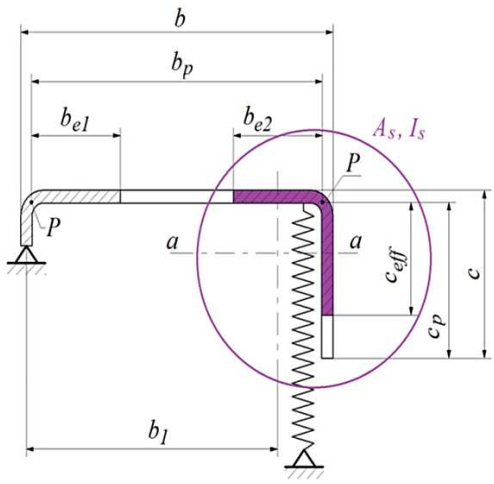



Fig. 2: Flange plane element of the CFS lipped channel stiffened by the single edge fold.

Let us introduce in the plane of thin-walled cross-section a Cartesian coordinate system $y_cOz_c$ with the origin in the center of mass *C* of the section, the direction of the coordinate system axes $y_cOz_c$ coincides with the direction of principle axes of inertia. Let us also describe the considered section of thin-walled bar by a set of sectional points **P** = {**p**$_j$ = {$y_j$,$z_j$} | $j = \overline{0, n}$} $y_j$ and $z_j$ are the coordinates of $j^{th}$ sectional point in the coordinate system $y_cOz_c$ introduced above) and by a set of sectional segments **S** = {**s**$_i$ = {**p**$_{i-1}$,**p**$_i$} | $i = \overline{1, n}$}, which connect to adjacent sectional points, where *n* is quantity of the sectional segments and *n* + 1 is quantity of the sectional points. It should be noted that the coordinates of the sectional points depend on the design variables of the formulated optimization problem **P** = **P**($\vec{X}$).

The following integral geometrical properties of considered cross-section can be calculated on the determined set **P** of sectional points and set **S** of sectional segments (see Annex C [22]): $A_g$ is the gross cross-sectional area; $I_y$ , $I_z$ are the second moments of inertia relative to the main axis of inertia, which coincide with the axes of global Cartesian coordinate system $y_cOz_c$; $i_y$, $i_z$ are the radiuses of inertia relative to the main axis of inertia; $I_\omega$ is the sectorial moment of inertia; $I_1$ is the second moment

of area for pure torsion. As the coordinates of the sectional points depend on the design variables, then the integral geometrical properties of the gross cross-section depends on the design variables as well.

Design sizes of plane cross-sectional elements (Fig. 1) for CFS lipped channel structural member are calculated according to [22] depending on the design variables *h, b* and *c* as well as on the constant internal bend radios *r* and profile thickness *t* as presented below:

$$h_p = h - 2R + r_m\sqrt{2}\,, \tag{4}$$

$$b_p = b - 2R + r_m\sqrt{2}\,, \tag{5}$$

$$c_p = c - R + r_m\frac{\sqrt{2}}{2}\,, \tag{6}$$

where $h_p$ is the design web height; $b_p$ is the design flange width; $c_p$ is the design length of a single edge fold; $r_m$ is the middle bend radius, $r_m = r + 0.5t$; $R$ is the external bend radius, $R = r + 1$.

Relative slenderness $\bar{\lambda}_{ph}$ of the web, relative slenderness $\bar{\lambda}_{pb}$ of the flanges and relative slenderness $\bar{\lambda}_{pc}$ of the single edge fold for CFS lipped channel are calculated according to [22, 23] as follow:

$$\bar{\lambda}_{ph} = \frac{h_p}{56.8t\varepsilon}\,, \tag{7}$$

$$\bar{\lambda}_{ph} = \frac{b_p}{56.8t\varepsilon}\,, \tag{8}$$

$$\bar{\lambda}_{pc} = \frac{c_p}{28.4t\varepsilon\sqrt{\tilde{\boldsymbol{k}}_{\boldsymbol{\sigma c}}(c_p/b_p)}}\,, \tag{9}$$

where $\varepsilon$ is material factor, $\varepsilon = \sqrt{235/f_{yb}}$ [MPa]; $\tilde{\boldsymbol{k}}_{\boldsymbol{\sigma c}}(c_p/b_p)$ is buckling factor calculated according to the dependency proposed by [22].

Cross-section flanges and web of CFS lipped channel structural member are subjected to post-buckling behavior (when local buckling occurs) in the case when its slenderness exceed limit value, namely web slenderness $\bar{\lambda}_{ph} > 0.673$ and/or flange slenderness $\bar{\lambda}_{pb} > 0.673$. In this case effective widths of the web $h_{eff}$ and flanges $b_{eff}$ as well as effective cross-sectional sizes $h_{e1}$, $h_{e2}$, $b_{e1}$, $b_{e2}$ are defined according to [22, 23] as presented below:

$$h_{e1} = h_{e2} = \frac{h_{eff}}{2} = \frac{h_p}{2\bar{\lambda}_{ph}}\left(1 - \frac{0.22}{\bar{\lambda}_{ph}}\right) = 28.4t\varepsilon\left(1 - \frac{12.496t\varepsilon}{h_p}\right) - if\ \bar{\lambda}_{ph} > 0.673, \tag{10}$$

$$h_{e1} = h_{e2} = \frac{h_p}{2} \text{ - otherwise} \tag{11}$$

$$b_{e1} = \frac{b_{eff}}{2} = \frac{b_p}{2\bar{\lambda}_{pb}}\left(1 - \frac{0.22}{\bar{\lambda}_{pb}}\right) = 28.4t\varepsilon\left(1 - \frac{12.496t\varepsilon}{b_p}\right) - if\ \bar{\lambda}_{ph} > 0.673, \tag{12}$$

$$b_{e2} = \frac{b_{eff}}{2} = \frac{b_p}{2\bar{\lambda}_{pb}\sqrt{\chi_d}}\left(1 - \frac{0.22}{\bar{\lambda}_{pb}\sqrt{\chi_d}}\right) = \frac{28.4t\varepsilon}{\sqrt{\chi_d}}\left(1 - \frac{12.496t\varepsilon}{b_p\sqrt{\chi_d}}\right) - if\ \bar{\lambda}_{ph} > 0.673, \tag{13}$$

$$b_{e1} = b_{e2} = \frac{b_p}{2} \text{ - otherwise,} \tag{14}$$

where $\chi_d$ is the reduction factor for the distortional buckling cross-section resistance calculated as presented below.

Single edge fold of CFS lipped channel cross-section is subjected to post-buckling behavior (when local buckling occurs) in case when it slenderness exceeds limit value ($\bar{\lambda}_{pc} > 0.748$). In this case effective single edge fold width $c_{eff}$ is determined according to [22] as follow:

$$c_{eff} = \frac{c_p}{\bar{\lambda}_{pc}\sqrt{\chi_d}}\left(1 - \frac{0.188}{\bar{\lambda}_{pc}\sqrt{\chi_d}}\right) = \frac{28.4t\varepsilon}{\sqrt{\chi_d}}\sqrt{\tilde{\boldsymbol{k}}_{\boldsymbol{\sigma c}}(c_p/b_p)}\left(1 - \frac{5.339t\varepsilon}{c_p\sqrt{\chi_d}}\sqrt{\tilde{\boldsymbol{k}}_{\boldsymbol{\sigma c}}(c_p/b_p)}\right) - if\ \bar{\lambda}_{ph} > 0.673, \tag{15}$$

$c_{eff} = c_p$ – otherwise. (16)

Let us also describe the considered effective cross-section of thin-walled bar by a set of sectional points $\mathbf{P}_{eff} = \{\mathbf{P}_{eff,j} = \{y_{eff,j}, z_{eff,j}\} \mid j = \overline{0, n_{eff}}\}$ ($y_{eff,j}$ and $z_{eff,j}$ are the coordinates of $j^{th}$ sectional point in the coordinate system $y_cOz_c$ introduced above) and by a set of sectional segments $\mathbf{S}_{eff} = \{\mathbf{S}_{eff,i} = \{\mathbf{P}_{eff,i-1}, \mathbf{P}_{eff,i}\} \mid i = \overline{1, n_{eff}}\}$, which connect to adjacent sectional points, where $n_{eff}$ is quantity of the sectional segments and $n_{eff}$ + 1 is quantity of the sectional points. It should be noted that the coordinates of the sectional points depend on the design variables of the formulated optimization problem as well as on the effective cross-sectional sizes $h_{e1}$, $h_{e2}$, $b_{e1}$, $b_{e2}$, $c_{eff}$: $\mathbf{P}_{eff} = \mathbf{P}_{eff}(\vec{X}, h_{e1}, h_{e2}, b_{e1}, b_{e2}, c_{eff})$.

The area $A_{eff}$ of the effective cross-section of CFS lipped channel structural member subjected to axial compression can be calculated on the determined set $\mathbf{P}_{eff}$ of sectional points and set $\mathbf{S}_{eff}$ of sectional segments (see Annex C [22]). As the coordinates of the effective cross-sectional points depend on the design variables, then the area $A_{eff}$ of the effective cross-section of CFS lipped channel structural member subjected to axial compression depends on the design variables as well.

Single edge folds in CFS lipped channel structural members ensure partial restraint for plane flanges. In order to estimate such restraint, the design cross-section of the stiffener (Fig. 2) should be introduced into the further consideration. The design cross-section of the stiffener consists of single edge fold with effective width $c_{eff}$ together with effective adjacent part of the flange with effective width $b_{e2}$ the thickness of the stiffener's design cross-section is equals to the profile thickness $t$ in case when the distortional buckling does not occur ($\chi_d = 1$). Otherwise, the reduced thickness $t_{red}$ of the stiffener's design cross-section allowing for reduced stiffener resistance due to flexural buckling of the stiffener is determined according to [22] as follow:

$$t_{red} = X_d^t. \quad (17)$$

Let us also describe the design cross-section of the stiffener by a set of sectional points $\mathbf{P}_s = \{\mathbf{P}_{s,j} = \{y_{s,j}, z_{s,j}\} \mid j = \overline{0, n_s}\}$ ($y_{z,j}$ and $z_{z,j}$ are the coordinates of $j^{th}$ sectional point in the coordinate system $y_cOz_c$ introduced above) and by a set of sectional segments $\mathbf{S}_s = \{\mathbf{S}_{s,i} = \{\mathbf{P}_{s,i-1}, \mathbf{P}_{s,i}\} \mid i = \overline{1, n_s}\}$, which connect to adjacent sectional points, where $n_s$ is quantity of the sectional segments and $n_s$ + 1 is quantity of the sectional points. It should be noted that the coordinates of the sectional points depend on the design variables of the formulated optimization problem as well as on the effective cross-sectional sizes $b_{e2}$, $c_{eff}$ and reduced thickness $t_{red}$ : $\mathbf{P}_s = \mathbf{P}_s(\vec{X}, b_{e2}, c_{eff}, t_{red})$.

The following geometrical properties of the design cross-section of the stiffener can be calculated on the determined set $\mathbf{P}_s$ of sectional points and set $\mathbf{S}_s$ of sectional segments: $A_s$ is the area of the stiffener's design cross-section; $I_s$ is the second moment of inertia for the stiffener's design cross-section; $b_{c,s}$ is the distance from the web-to-flange junction to the gravity center of the effective area of the edge stiffener.

The partial restraint for plane flanges provided by the single edge folds in CFS lipped channel structural members can be simulated using a linear spring. In case of the axial compression stiffness for such a linear spring can be estimated according to [22] as presented below:

$$K = \frac{E}{3.64} \cdot \frac{t^3}{b_{c,s}^2(b_{c,s}+1.5h-3t)}. \quad (18)$$

It should be noted that analytical expression for stiffness of the linear spring presented above is restricted by the case of cold-formed structural members with flanges stiffened by single or double edge folds only and cross-section symmetrical relatively to the main axes of inertia which is perpendicular to the web plane.

Then relative slenderness of the stiffener $\bar{\lambda}_d$ corresponded to the flexural buckling of the stiffener is calculated according to [22] as follow:

$$\bar{\lambda}_d = \sqrt{\frac{f_{yb}A_s}{2\sqrt{KEI_s}}}. \quad (19)$$

The reduction factor $\chi_d$ for the flexural buckling of the stiffener (or reduction factor for the distortional buckling cross-section resistance) is determined iteratively depending on relative slenderness $\bar{\lambda}_d$ using dependency (5.12) proposed by [22]:

$$X_d = \equiv (\bar{\lambda}_d). \tag{20}$$

The maximization criterion of the minimum design buckling resistance of the structural member subjected to axial compression can be considered as the purpose function (2) of the optimization problem and can be written as follow:

$$N_{bRd,min} = min(N_{byRd}, N_{bzRd}, N_{bT,Rd}, N_{bTF,Rd}) \rightarrow max, \tag{21}$$

where $N_{bRd,min}$ is the minimum design buckling resistance; $N_{byRd}$, $N_{bzRd}$ are the design buckling resistance for flexural buckling of the cold-formed structural member relative to the main axis of inertia *y - y* and *z - z* determined according to [22, 24]; $N_{bT,Rd}$, $N_{bTF,Rd}$ are the design buckling resistance corresponded to the torsional and flexural-torsional buckling of the structural member calculated according to [22,24]. Then the purpose function can be rewritten as follow:

$$N_{bRd,min} = \frac{A_{eff} f_{yb}}{\gamma_{M1}} \times min\{X_y, X_z, X_T, X_{TF}\} \rightarrow max, \tag{22}$$

where $\chi_y$, $\chi_z$, $\chi_T$, $\chi_{TF}$ are buckling factors allowing for the flexural buckling of the CFS structural member relative to the main axis of inertia *y - y* and *z - z,* as well as for the torsional and flexural-torsional buckling. The buckling factors $\chi_y$, $\chi_z$, $\chi_T$, $\chi_{TF}$ are determined from the relevant buckling curve *b* according to [22, 24] as:

$$X = \left(0.466 + 0.17\bar{\lambda} + 0.5\bar{\lambda}^2 + \sqrt{(0.466 - 0.83\bar{\lambda} + 0.5\bar{\lambda}^2)(0.466 + 1.17\bar{\lambda} + 0.5\bar{\lambda}^2)}\right)^{-1} \leq 1.0, \tag{23}$$

with substitution of the relevant non-dimensional slendernesses $\bar{\lambda}_y$, $\bar{\lambda}_z$, $\bar{\lambda}_T$, $\bar{\lambda}_{TF}$ corresponded to the considered buckling modes and calculated taking into account geometrical properties of the effective cross-section of the structural member subjected to the axial compression according to [22, 24] as presented below:

$$\bar{\lambda} = \sqrt{\frac{A_{eff} f_{yb}}{N_{cr}}}, \tag{24}$$

where $N_{cr}$ is the elastic critical force for the relevant buckling mode calculated taking into account gross cross-section geometrical properties of the structural member according to [29]. The non-dimensional slendernesses $\bar{\lambda}_y$, $\bar{\lambda}_z$, $\bar{\lambda}_T$, $\bar{\lambda}_{TF}$ are determined with substitution in (24) instead of $N_{cr}$ the corresponded elastic critical force $N_{cr,y}$, $N_{cr,z}$, $N_{cr,T}$ or $N_{cr,TF}$ here $N_{cr,y}$ and $N_{c,z}$ are the elastic critical forces for the flexural buckling mode relative to the main axes of inertia *y - y* and *z - z* respectively; $N_{cr,T}$, $N_{cr,TF}$ are the elastic critical forces for the torsional and torsional-flexural buckling mode respectively.

System of constraints (3) for the formulated optimization problem consists of a constraint on the profile perimeter or on a strip width which can be written as presented below:

$$\frac{h+2b+2c}{P_{max}} - 1 \leq 0, \tag{25}$$

where $P_{max}$ is the maximum value of the cross-section perimeter for CFS lipped channel.

The constraints reflected design code requirements [22] for the ultimate slenderness of the cross-section elements of the CFS channel with flanges stiffened by single edge folds are also included in the system of constraints (3) and presented below:

$$\frac{h}{500r} - 1 \leq 0, \tag{26}$$

$$\frac{b}{60t} - 1 \leq 0, \tag{27}$$

$$\frac{c}{50t} - 1 \leq 0, \tag{28}$$

$$0.2 - \frac{c}{b} \leq 0, \tag{29}$$

$$\frac{c}{b} - 0.6 \leq 0, \tag{30}$$

Additionally, a constraint on the minimum gap between single edge folds ends allowing for providing an access to the internal surface of the CFS lipped channel (for example, in order to organize a bolted connection on the profile flanges) is included to the system of constraints (3) as well and written as below:

$$\frac{h-2c}{d_{min}} - 1 \leq 0, \tag{31}$$

where $d_{min}$ is the minimum gap between single edge folds ends.

Thus, the optimization problem of cross-sectional sizes for CFS lipped channel structural member subjected to axial compression is formulated as follow: to find optimum cross-sectional sizes of CFS lipped channel (web height *h*, flange width *b* and single edge fold length *c*) providing the maximum value of the determined objective function (21) in the feasible region defined by the system of constraints (25) – (31) when the profile perimeter (strip width), profile thickness, design lengths of the structural member as well as material properties are constant and specified in advance.

## 3 Optimization results

The following CFS lipped channels from the whole profile assortment range manufactured by the company Blachy Pruszyński have been chosen to further optimization: C 100 × 48 × 18 and C 100 × 60 × 19 [25]. Other lipped channels have the same flange widths (48 mm and 60 mm) and have deeper web height simultaneously indicating their more rational usage as beam-column or beam structural members. The strip widths for the chosen CFS lipped channels are 23.2 cm and 25.8 cm respectively.

The following design flexural buckling length has been considered as initial data for optimization: 1.5 m, 2.0 m and 2.5 m. The use of single profiles for long-length CFS structural member with the design length greater than 2.5 m as well as short-length CFS structural members with the design length smaller than 1.5 m is not rational.

Taking into account it small dimensionality the formulated parametric optimization problem has been solved by exhaustive search method using the software written in Python. As optimization results the CFS lipped channels with optimum cross-sectional dimensions have been obtained depending on the profile thickness and design lengths of the structural member. The obtained CFS lipped channel structural members with optimum cross-sectional sizes have higher design buckling resistance under the central compression comparing with the CFS lipped channels with the same stripe width proposed by the manufacturer [25]. The increasing of the load-carrying capacity up to and including 12.14 % (for the strip width 23.2 cm) and 19.01 % (for the strip width 25.8 cm) has been achieved.

Table 1: CFS lipped channel structural members with optimum cross-sectional sizes (strip width is $P_{max}$ = 23.2 cm corresponded to initial profile C 100 × 48 × 18).

| Design buckling length [m] | *t* [cm] | Optimum cross-sectional sizes [cm] | $N_{bRd,min,}$ [kN] | Buckling mode | Web local buckling | Flange local buckling | Distor-sional buckling | Load-carrying capacity increasing [%] |
|---|---|---|---|---|---|---|---|---|
| 1.5 | 0.100 | 8.8 × 4.5 × 2.7 | 31.696 | tors. - flex. | Yes | Yes | Yes | 12.14 |
| | 0.125 | 8.8 × 4.5 × 2.7 | 41.871 | tors. - flex. | Yes | Yes | Yes | 10.81 |
| | 0.150 | 8.8 × 4.5 × 2.7 | 51.664 | tors. - flex. | Yes | No | Yes | 9.65 |
| | 0.175 | 9.8 × 4.2 × 2.5 | 63.914 | tors. - flex. | Yes | No | No | 12.66 |
| | 0.200 | 9.8 × 4.2 × 2.5 | 73.285 | tors. - flex. | Yes | No | No | 10.92 |
| | 0.225 | 9.8 × 4.2 × 2.5 | 82.890 | tors. - flex. | Yes | No | No | 9.40 |
| | 0.250 | 9.6 × 4.3 × 2.5 | 92.140 | tors. - flex. | Yes | No | No | 5.55 |
| | 0.275 | 9.6 × 4.3 × 2.5 | 102.099 | flex. minor axis | Yes | No | No | 5.88 |
| | 0.300 | 9.2 × 4.4 × 2.6 | 111.737 | tors. - flex. | No | No | No | 3.37 |

Table 2 (continuation): CFS lipped channel structural members with optimum cross-sectional sizes (strip width is $P_{max}$ = 23.2 cm corresponded to initial profile C 100 × 48 × 18).

| Design buckling length [m] | *t* [cm] | Optimum cross-sectional sizes [cm] | $N_{bRd,min,}$ [kN] | Buckling mode | Web local buckling | Flange local buckling | Distor-sional buckling | Load-carrying capacity increasing [%] |
|---|---|---|---|---|---|---|---|---|
| 2.0 | 0.100 | 9.8 × 4.2 × 2.5 | 21.941 | tors. - flex. | Yes | Yes | Yes | 11.04 |
| | 0.125 | 9.8 × 4.2 × 2.5 | 28.539 | tors. - flex. | Yes | Yes | Yes | 10.32 |
| | 0.150 | 9.8 × 4.2 × 2.5 | 35.164 | tors. - flex. | Yes | No | Yes | 9.50 |
| | 0.175 | 9.8 × 4.2 × 2.5 | 43.189 | tors. - flex. | Yes | No | No | 11.35 |
| | 0.200 | 9.6 × 4.3 × 2.5 | 49.898 | tors. - flex. | Yes | No | No | 9.38 |
| | 0.225 | 9.2 × 4.4 × 2.6 | 56.837 | tors. - flex. | Yes | No | No | 7.30 |
| | 0.250 | 9.2 × 4.4 × 2.6 | 64.433 | flex. minor axis | Yes | No | No | 5.03 |
| | 0.275 | 9.0 × 4.5 × 2.6 | 71.707 | tors. - flex. | No | No | No | 3.04 |
| | 0.300 | 9.0 × 4.6 × 2.5 | 78.879 | flex. minor axis | No | No | No | 1.26 |
| 2.5 | 0.100 | 9.8 × 4.2 × 2.5 | 15.699 | tors. - flex. | Yes | Yes | Yes | 10.72 |
| | 0.125 | 9.8 × 4.2 × 2.5 | 20.445 | tors. - flex. | Yes | Yes | Yes | 10.11 |
| | 0.150 | 9.8 × 4.2 × 2.5 | 25.446 | tors. - flex. | Yes | No | Yes | 9.39 |
| | 0.175 | 9.6 × 4.3 × 2.5 | 31.099 | tors. - flex. | Yes | No | No | 9.53 |
| | 0.200 | 9.2 × 4.4 × 2.6 | 36.385 | tors. - flex. | Yes | No | No | 7.22 |
| | 0.225 | 9.2 × 4.5 × 2.5 | 41.836 | flex. minor axis | Yes | No | No | 4.39 |
| | 0.250 | 9.4 × 4.7 × 2.2 | 47.263 | tors. - flex. | Yes | No | No | 1.18 |
| | 0.275 | 9.8 × 5.0 × 1.7 | 53.058 | tors. - flex. | Yes | No | No | 5.36 |
| | 0.300 | 9.2 × 5.0 × 2.0 | 59.257 | flex. minor axis | No | No | No | 9.68 |

Table 3: CFS lipped channel structural members with optimum cross-sectional sizes (strip width is $P_{max}$ = 25.8 cm corresponded to initial profile C100 × 60 × 19).

| Design buckling length [m] | *t* [cm] | Optimum cross-sectional sizes [cm] | $N_{bRd,min,}$ [kN] | Buckling mode | Web local buckling | Flange local buckling | Distor-sional buckling | Load-carrying capacity increasing [%] |
|---|---|---|---|---|---|---|---|---|
| 1.5 | 0.100 | 9.8 × 5.0 × 3.0 | 37.761 | tors. - flex. | Yes | Yes | Yes | 18.80 |
| | 0.125 | 9.8 × 5.0 × 3.0 | 50.890 | tors. - flex. | Yes | Yes | Yes | 17.31 |
| | 0.150 | 9.8 × 5.0 × 3.0 | 64.073 | tors. - flex. | Yes | Yes | Yes | 16.32 |
| | 0.175 | 10.8 × 4.7 × 2.8 | 80.942 | tors. - flex. | Yes | No | No | 19.66 |
| | 0.200 | 10.8 × 4.7 × 2.8 | 92.314 | tors. - flex. | Yes | No | No | 17.72 |
| | 0.225 | 10.8 × 4.7 × 2.8 | 103.775 | tors. - flex. | Yes | No | No | 16.20 |
| | 0.250 | 10.8 × 4.7 × 2.8 | 115.367 | tors. - flex. | Yes | No | No | 14.88 |
| | 0.275 | 10.8 × 4.7 × 2.8 | 127.125 | tors. - flex. | Yes | No | No | 13.71 |
| | 0.300 | 10.8 × 4.7 × 2.8 | 139.079 | tors. - flex. | Yes | No | No | 12.83 |
| 2.0 | 0.100 | 9.8 × 5.0 × 3.0 | 27.611 | tors. - flex. | Yes | Yes | Yes | 18.71 |
| | 0.125 | 10.8 × 4.7 × 2.8 | 36.181 | tors. - flex. | Yes | Yes | Yes | 17.97 |
| | 0.150 | 10.8 × 4.7 × 2.8 | 44.738 | tors. - flex. | Yes | No | Yes | 17.22 |
| | 0.175 | 11.4 × 4.5 × 2.7 | 55.376 | flex. minor axis | Yes | No | No | 19.60 |
| | 0.200 | 10.8 × 4.7 × 2.8 | 63.852 | tors. - flex. | Yes | No | No | 18.44 |
| | 0.225 | 10.8 × 4.7 × 2.8 | 72.675 | tors. - flex. | Yes | No | No | 17.50 |
| | 0.250 | 10.6 × 4.8 × 2.8 | 81.223 | tors. - flex. | Yes | No | No | 15.96 |
| | 0.275 | 10.6 × 4.8 × 2.8 | 90.040 | flex. minor axis | Yes | No | No | 14.45 |
| | 0.300 | 10.2 × 4.9 × 2.9 | 99.673 | tors. - flex. | Yes | No | No | 13.51 |
| 2.5 | 0.100 | 10.8 × 4.7 × 2.8 | 20.192 | tors. - flex. | Yes | Yes | Yes | 19.01 |
| | 0.125 | 10.8 × 4.7 × 2.8 | 26.228 | tors. - flex. | Yes | Yes | Yes | 18.53 |
| | 0.150 | 10.8 × 4.7 × 2.8 | 32.448 | tors. - flex. | Yes | No | Yes | 17.96 |
| | 0.175 | 10.8 × 4.7 × 2.8 | 39.897 | tors. - flex. | Yes | No | No | 19.40 |
| | 0.200 | 10.8 × 4.7 × 2.8 | 46.532 | flex. minor axis | Yes | No | No | 18.38 |
| | 0.225 | 10.6 × 4.8 × 2.8 | 53.195 | flex. minor axis | Yes | No | No | 16.85 |
| | 0.250 | 10.2 × 4.9 × 2.9 | 60.157 | tors. - flex. | Yes | No | No | 15.22 |
| | 0.275 | 10.0 × 5.0 × 2.9 | 67.017 | tors. - flex. | Yes | No | No | 12.97 |
| | 0.300 | 10.0 × 5.1 × 2.8 | 74.037 | flex. minor axis | Yes | No | No | 10.62 |

Table 1 and Table 2 present the optimum cross-sectional sizes for CFS lipped channel structural members depending on the profile thickness as well as on the different design lengths corresponded to the flexural buckling modes. As you can see from the Table 1 and Table 2 the torsional-flexural buckling resistance of CFS lipped channel structural members has been determinative for the majority of the optimum decisions. Web local buckling phenomenon has been occurred in all obtained CFS lipped channel cross-sections with optimum sizes. Flange local buckling phenomenon as well as distortional buckling phenomenon has been occurred in obtained optimum CFS lipped channel cross-sections with small profile thicknesses only (up to and including 0.15 mm – for flange local buckling phenomenon and 0.175 mm – distortional buckling phenomenon).

As you can see from Table 1 and Table 2 the optimum length of the single edge fold in all optimum CFS lipped channel cross-sections is greater comparing with the single edge fold length of CFS lipped channels proposed by the manufacturer. The average optimum ratio of the single edge fold length to the flange width *c/b* has been obtained as 0.58. The average optimum ratio of the flange width to the web height *b/h* has been received equal to 0.46. The optimum ratio between the second moments of inertia relatively to the minor and major axis of inertia respectively has been received for all optimum solutions in range 0.2…0.29 due to the type of the cross-section and post-buckling behavior of the lipped channel web. The radiuses of inertia with respect to the main axes of inertia have been obtained for all CFS lipped channel with optimum cross-sectional dimensions as follow: $i_y$ = (0.38 ... 0.39)*h,* $i_z$ = (0.37 ... 0.41)*b.*

It should be noted, that the optimum solutions has been obtained using the maximization criterion for the minimum design buckling resistance calculated for pure axial compression without additional bending moments due to the eccentricity of the centroidal axis of the effective section. Taking into account the eccentricity in scope of the optimization procedure can be considered by further investigations.

Additionally, in order to obtain optimum solutions for cross-sectional dimensions of the CFS lipped channel structural members which are independent from the design flexural lengths and profile thickness, a searching problem for a compromise solutions can be stated and considered in future study.

## 4 Conclusion

Searching for optimum cross-sectional sizes of CFS lipped channel structural members taking into account post-buckling behavior and structural requirements has been realized. The obtained CFS lipped channel structural members with optimum cross-sectional sizes have higher design buckling resistance under the axial compression comparing with the CFS lipped channels with the same stripe width proposed by the manufacturer.

The torsional-flexural buckling resistance of CFS lipped channel structural members has been determinative for the majority of the optimum decisions. Web local buckling phenomenon has been occurred in all obtained CFS lipped channel cross-sections with optimum sizes. The optimum length of the single edge fold in all optimum CFS lipped channel cross-sections was greater comparing with the single edge fold length of CFS lipped channels proposed by the manufacturer.

Presented results of the performed optimization calculation allow developing guides for designers relating to the optimum material distribution in the cross-sections of CFS structural members as well as are base to develop effective national ranges of assortments of cold-formed profiles.

## References

[1] BILYK, S. I. – YURCHENKO, V. V.: Size optimization of single edge folds for cold-formed structural members. Strength of Materials and Theory of Structures: Scientific-and-technical collected articles, Kyiv: KNUBA, Iss. 105, 2020, pp. 73-86, DOI: 10.32347/2410-2547.2020.105.73-86.

[2] MOJTABAEI, S. M. – BECQUE, J. – HAJIRASOULIHA, I.: Structural size optimization of single and built-up cold-formed steel beam-column members. Journal of Structural Engineering, Vol. 147, Iss. 4, 2021, art. 04021030, DOI: 10.1061/(asce)st.1943-541x.0002987.

[3] LENG, J.: Optimization Techniques for Structural Design of Cold-Formed Steel Structures. Recent Trends in Cold-Formed Steel Construction, Elsevier, 2016, pp. 129–151.

[4] LIANG, H. – ROY, K. – FANG, Z. – LIM, J. B. P.: A Critical Review on Optimization of Cold-Formed Steel Members for Better Structural and Thermal Performances. Buildings, Vol. 12 (1), 2022, 29 p., DOI: 10.3390/buildings12010034.

[5] AMMASH, H. K.: Shape optimization of innovation cold-formed steel columns under uniaxial

compressive loading. Jordan Journal of Civil Engineering, Vol. 11, Iss. 3, 2017, pp. 473-489.
[6] LENG, J. – GUEST, J. K. – SCHAFER, B. W.: Shape optimization of cold-formed steel columns. Thin-Walled Structures, Vol. 49, 2011, pp. 1492–1503, DOI: 10.1016/j.tws.2011.07.009.
[7] LENG, J. - LI, Z. - GUEST, J. K. - SCHAFER, B. W.: Shape optimization of cold-formed steel columns with fabrication and geometric enduse constraints. Thin-Walled Structures, Vol. 85, 2014, pp. 271–290, DOI: 10.1016/j.tws.2014.08.014.
[8] WANG, B. - GILBERT, B. P. - GUAN, H. - TEH, L. H.: Shape optimisation of manufacturable and usable cold-formed steel singly-symmetric and open columns. Thin-Walled Structures, Vol. 109, 2016, pp. 271–284, DOI: 10.1016/j.tws.2016.10.004
[9] YE, J. - HAJIRASOULIHA, I. -BECQUE, J. - PILAKOUTAS, K.: Development of more efficient cold-formed steel channel sections in bending. Thin-Walled Structures, Vol. 101, 2016, pp. 1–13, DOI: 10.1016 /j.tws.2015.12.021.
[10] GATHEESHGAR, P. – POOLOGANATHAN, K. – GUNALAN, S. – SHYHA, I. – TSAVDARIDIS, K. D. – CORRADI, M.: Optimal design of cold-formed steel lipped channel beams: Combined bending, shear, and web crippling. Structures, Vol. 28, 2020, pp. 825–836, DOI: 10.1016/j.istruc.2020.09.027.
[11] LEE, J. – KIM, S. M. – PARK, H. S. – WOO, B. H.: Optimum design of cold-formed steel channel beams using micro Genetic Algorithm. Engineering Structures, Vol. 27, 2005, pp. 17–24, DOI: 10.1016/j.engstruct.2004.08.008.
[12] MOJTABAEI, S. M. – YE, J. – HAJIRASOULIHA, I.: Development of optimum cold-formed steel beams for serviceability and ultimate limit states using Big Bang-Big Crunch optimisation. Engineering Structures, Vol. 195, 2019, pp. 172–181, DOI: 10.1016/j.engstruct.2019.05.089
[13] GATHEESHGAR, P. – POOLOGANATHAN, K. – GUNALAN, S. – TSAVDARIDIS, K. D. – NAGARATNAM, B. – IACOVIDOU, E.: Optimised cold-formed steel beams in modular building applications. Journal of Building Engineering, Vol. 32, 2020, 18 p., DOI: 10.1016/j.jobe.2020. 101607.
[14] MA, W. – BECQUE, J. – HAJIRASOULIHA, I. – YE, J.: Cross-sectional optimization of cold-formed steel channels to Eurocode 3. Engineering Structures, Vol. 101, 2015, pp. 641–651, DOI: 10.1016/j.engstruct.2015.07.051.
[15] PARASTESH, H. – HAJIRASOULIHA, I. – TAJI, H. – BAGHERI SABBAGH, A.: Shape optimization of cold-formed steel beam-columns with practical and manufacturing constraints. Journal of Constructional Steel Research, Vol. 155, 2019, pp. 249–259, DOI: 10.1016/j. jcsr.2018.12.031.
[16] WANG, B. - BOSCO, G. L. - GILBERT, B. P. - GUAN, H. - TEH, L. H.: Unconstrained shape optimisation of singly-symmetric and open cold-formed steel beams and beam-columns. Thin-Walled Structures, Vol. 104, 2016, pp. 54–61, DOI: 10.1016/j.tws.2016.03.007.
[17] PARASTESH, H. – M. MOJTABAEI, S. – TAJI, H. – HAJIRASOULIHA, I. – B. SABBAGH, A.: Constrained optimization of anti-symmetric cold-formed steel beam-column sections. Engineering Structures, Vol. 228, 2021, 16 p., DOI: 10.1016/j.engstruct.2020.111452.
[18] YURCHENKO, V. – PELESHKO, I.: Improved gradient projection method for parametric optimisation of bar structures. Magazine of Civil Engineering, Vol. 98, Iss. 6, 2020, 16 p., DOI: 10.18720/MCE. 98.12.
[19] YURCHENKO, V. V. – PELESHKO, I. D.: Searching for optimal pre-stressing of steel bar structures based on sensitivity analysis. Archives of Civil Engineering, Vol. 66, No. 3, 2020, pp. 525-540, DOI: 10.24425/ACE.2020.134411.
[20] NIKOLIĆ, R. R. – DJOKOVIĆ, J. M. – BUJŇÁK, J.: Optimization of the sandwich column with the truss core which is subjected to the compressive loading. Civil and Environmental Engineering, Vol.12, Iss.1, 2016, pp .47-54, DOI: 10.1515/cee-2016-0007.
[21] PERMYAKOV, V. O. – YURCHENKO, V. V. – PELESHKO, I. D.: An optimum structural computer-aided design using hybrid genetic algorithm. Proceeding of the International Conference Progress in Steel, Composite and Aluminium Structures, 2006, pp. 819-826.
[22] EN 1993-1-3:2006: EuroCode 3: Design of steel structures - Part 1-3: General rules – Supplementary rules for cold-formed members and sheeting.
[23] EN 1993-1-5:2006: EuroCode 3: Design of steel structures - Part 1-5: General rules – Plated structural elements.
[24] EN 1993-1-1:2005: EuroCode 3: Design of steel structures - Part 1-1: General rules and rules for buildings.
[25] Assortment ranges of the cold-formed profiles for light gauge steel structures of the Ukrainian manufacturers. UCSC-014-16, 2016. 32 p. (in Ukrainian).